

Nondestructive readout for a superconducting flux qubit

A. Lupascu, C. J. M. Verwijs, R. N. Schouten, C. J. P. M. Harmans, and J. E. Mooij
 Department of NanoScience, Delft University of Technology,
 PO Box 5046, 2600 GA Delft, The Netherlands
 (Dated: May 22, 2019)

We have implemented a nondestructive method for the readout of a flux qubit. The detection is based on the measurement of the Josephson inductance of a DC superconducting quantum interference device (DC-SQUID) inductively coupled to the qubit. The SQUID is included in a resonant circuit, allowing for high flux sensitivity. The measurement strength can be tuned with the amplitude of the RF signal used to drive the resonant circuit. Using this method, we measured the spectroscopy of a persistent current qubit and we obtained relaxation times of the order of 80 s.

PACS numbers: 03.67.Lx, 85.25.Cp, 85.25.Dq

Various two level systems based on Josephson junctions have been proposed as possible basic units for a quantum information processor [1], due to the flexibility in their design parameters and scalability. These systems make use in different ways of the interplay between the Josephson energy and the charging energy for superconducting tunnel junctions circuits. Coherent evolution for single qubits was observed [2, 3, 4, 5, 6, 7], and dynamical [8, 9] and spectroscopic [10, 11] evidence for 2-qubits coupling was obtained. Flux-based qubits contain a superconducting loop interrupted by one or more Josephson junctions. If the magnetic flux threading the loop is close to an even number of half flux quanta, the two lowest energy eigenstates are characterized by different values of the persistent current in the loop.

A DC-SQUID magnetometer is commonly used to measure the state of a flux qubit. The flux generated by the qubit in the SQUID loop influences the Josephson coupling strength of the SQUID. This can be determined by measuring the maximum supercurrent [6]. However, switching to the voltage state causes strong disturbance to the circuit used to read the qubit state and to the qubit itself. This makes the switching current measurement method unsuitable for experiments in which the preservation of the qubit state after the measurement or performing correlation measurements on multiple qubits are required.

In this Letter, we describe a new way to use a SQUID for the readout of a flux qubit and we report the first experiments on spectroscopy and relaxation time measurements of such a qubit, that use this detection scheme. The value of the SQUID Josephson coupling strength is inferred on the basis of the directly measured value of the Josephson inductance $L_J = \phi_0/2 I_c$, where $\phi_0 = h/2e$ and I_c is the SQUID critical current. The value of the Josephson inductance can be determined by injecting an AC bias current with an amplitude small compared to the critical current, such that the SQUID remains in the superconducting state. If an AC current at frequency

is injected in the SQUID, the order of magnitude of the maximum voltage across the SQUID is ϕ_0 . The

achievable value of the relative change in the Josephson inductance corresponding to the change in qubit state is typically less than a few percent. In order to increase the difference in AC voltages corresponding to the two qubit states, the SQUID is inserted in a resonant circuit. For qubits based on charge states, detection schemes based on similar methods are the radio-frequency single electron tunnelling transistor [12] and the radio-frequency Bolzmann transistor electrometer [13].

In a basis formed of two states with different persistent currents, the evolution of a flux qubit is described by the Hamiltonian

$$H = \frac{1}{2} (\omega_z + \omega_x) : \quad (1)$$

Our flux qubit is a persistent current qubit (PCQ) [14]. It consists of a superconducting loop interrupted by three Josephson junctions. In the case of the PCQ, $\omega = 2I_p/(2n+1)\phi_0/2$ (n is integer), in which I_p is the persistent current of the qubit and ω is the externally imposed magnetic flux.

For our detection scheme, the amplitude of the AC voltage across the SQUID is averaged for a certain period of time. The measurement time is defined as the averaging time necessary for the uncertainty in the value of the voltage due to noise to be equal to the difference between the voltage values corresponding to the two qubit states. The measurement is efficient if the measurement time is much smaller than the qubit relaxation time due to the back-action of the detector. The SQUID back-action on the qubit during the measurement was calculated [15] assuming that the amplitude of the current in the SQUID is small enough not to drive it into the non-linear regime. It has been found that the most important contribution to decoherence is due to the mixing of noise in the circuit by the AC bias current used to excite the resonant circuit. The relaxation rate is given by

$$\Gamma = \frac{1}{2h^2} \sin^2 \left(\frac{e\omega}{2} \right) K^2 \left(\frac{e\omega}{2} \right) [S_e^+ (\omega_0 + \omega) + S_e^+ (\omega_0 - \omega)] : \quad (2)$$

In the above expression $\tan \theta = \omega_0 - \omega = \frac{p}{2} \frac{\omega_0}{\omega_0^2 + \omega^2} = \frac{p}{h}$, ω is the angular frequency of the circuit driving signal,

S^+ is the Fourier transform of the symmetrized correlation function of the phase operator ϕ (defined as the average of the phase differences across the two SQUID junctions) and $k(\phi_0)$ describes the coupling between the SQUID and the measured flux qubit. The function

$$k(\phi_0) = M I_p I_{\text{circ,squid}} \sin(\phi_0) \quad (3)$$

is the product of the qubit-SQUID mutual inductance M , qubit persistent current I_p , SQUID circulating current $I_{\text{circ,squid}}$ for vanishing bias current, given by $I_{\text{circ,squid}} \sin(\phi_{\text{qubit}} = 0)$ (in which $I_{\text{circ,squid}}$ is the value of the critical current of the SQUID junctions and ϕ_{qubit} is the external flux threading the SQUID loop) and the amplitude of the phase oscillations ϕ_0 . Further analysis for the type of detection circuit presented below shows that, if a low noise cryogenic amplifier is used, the state of the qubit can be read with large fidelity.

Figure 1 shows the schematic diagram of the circuit containing the PCQ, the readout device and the microwave excitation line. The combined qubit-SQUID system is fabricated on an oxidized silicon substrate using standard electron beam lithography and double-angle shadow evaporation of aluminum in situ. Two of the three qubit Josephson junctions have $E_c = 4.6$ GHz and $E_J = E_c = 110$. The third junction has a size smaller by a factor ≈ 0.75 . The areas of the qubit and SQUID are, respectively, $A = 100 \mu\text{m}^2$ and $A_{\text{qubit}} = 128 \mu\text{m}^2$. The chip containing the qubit and the SQUID is attached to a printed circuit board on which the capacitor C and the resistors R_1 , R_b and R_m are mounted. The capacitor C was positioned close to the SQUID in order to limit the value of the stray inductance L_s . The resistance R_1 is used to increase the quality factor of the resonant circuit to $Q \approx 40$, which would otherwise be small due to the small amplifier input impedance (50 Ω). Switching current measurements can also be performed by using, for low frequency current injection, the same line as used for the RF bias and measuring the voltage V_{DC} . The resistor R_b , in the bias line, and the resistor R_m are chosen large in comparison with the load resistor R_1 , so that the quality factor is not decreased significantly. The printed circuit board is mounted inside a Cu box, anchored at the mixing chamber of a dilution refrigerator. Qubit excitation is realized using a coaxial cable terminated in a low inductance line characterized by a mutual inductance to the qubit $M_{MW} = 0.12 \text{ pH}$. The filtering is realized using attenuators in the microwave excitation and bias lines, Cu powder filters in the bias and DC voltage measurement lines and an RC filter in the DC voltage measurement line.

Switching current measurements were used to characterize the SQUID [16]. The dependence of the average SQUID switching current on the magnetic field had a period $B_{\text{qubit}} = 16.1$ T. The RF transmission measurements displayed a peak at a frequency ω_0 , depending on the applied magnetic field. The position of the resonant

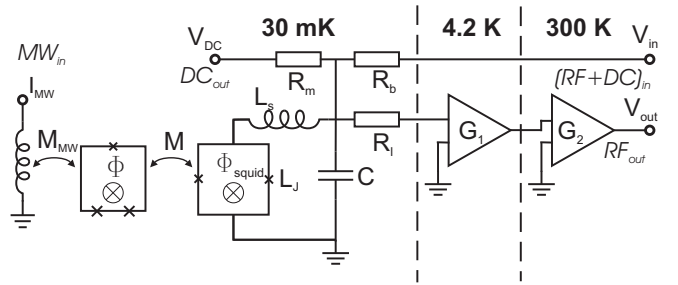


FIG. 1: A circuit diagram of the PCQ with the manipulation and readout circuit. The qubit is biased with a static magnetic flux, using an external coil, and with a small flux oscillating in the MW frequency range, using a small inductance coil. A coaxial line is used to apply the RF and DC bias current (for the inductance method and switching current measurements, respectively). The values of the components are $L_s = 2.35 \text{ nH}$, $C = 12 \text{ pF}$, $R_1 = 820 \Omega$, $R_b = 5.6 \text{ k}\Omega$ and $R_m = 11 \text{ k}\Omega$. The output RF signal is amplified at the 4.2 K and room temperature stages with gains $G_1 = 14 \text{ dB}$ and $G_2 = 70 \text{ dB}$, respectively.

peak as a function of the magnetic field has the same period as the SQUID modulation period and the maximum resonant frequency corresponds to the field where the average SQUID switching current is maximum, in agreement with the expected variation of the Josephson inductance. From the dependence of the resonance frequency on the magnetic field, the values $L_{J,m} \approx 0.31 \text{ nH}$ (the Josephson inductance at an integer number of flux quanta in the SQUID) and $L_s \approx 2.35 \text{ nH}$ are found. The value of $L_{J,m}$ is in quantitative agreement with independently measured circuit parameters.

In the analyzed magnetic field range, the SQUID modulation curve shows, at 6 positions, equidistant steps in the average switching current, with a period $B = 21 \text{ T}$. The fact that $B = B_{\text{qubit}} / A_{\text{qubit}} = A$ (indicating a period of 1 T in the qubit) and the variation of the average switching current is in the direction of increasing flux identify these features as consecutive qubit steps (regions around an odd multiple of $\phi_0 = 2\pi$, where the ground state expectation value of the qubit generated flux changes from negative to positive values). The measurements presented below were done at two different qubit step positions using the Josephson inductance measurement method. In order to obtain a high measurement efficiency we chose steps at $B = 0.623 \text{ T}$ and at $B = 63.674 \text{ T}$, separated by 3 T in the qubit (to be called in the following steps 1 and 2).

Figure 2a shows the resonance peak at the center of step 2. As the magnetic field is increased, the resonance frequency increases. At a fixed operating frequency at the left of the resonance peak, an increase in the magnetic field translates into a decrease in the output voltage, as opposed to the case of a frequency at the right of the resonance peak, when the output voltage is an increasing

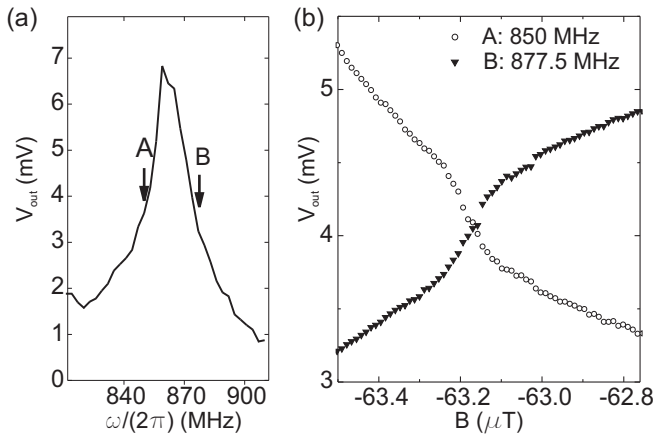


FIG. 2: (a) Frequency response of the readout circuit at a magnetic field corresponding to the qubit step 2. (b) The response to external flux changes for two operating frequencies, indicated by arrows in (a).

function of external field. For two values of the operating frequency, the dependence on the applied magnetic field is shown in Fig. 2b. The linear background is due to the external magnetic flux in the SQUID, whereas the steeper variation in the middle is due to the qubit persistent current in the ground state.

The spectroscopy and relaxation time measurements consist of the repetition of the following sequence: a microwave burst at frequency f_{MW} and power P_{MW} is used to excite the qubit (for a time T_{MW}) and, after a waiting time (T_d), the RF bias current used to excite the SQUID is applied for a time T_m . The measurement time, T_m , is chosen larger than the response time of the SQUID, $Q=10$. The output voltage V_{out} is averaged over typically 1000 repetitions of the described sequence.

Figure 3 shows the spectroscopy measurements results. For each value of the external magnetic field, the average value of the output voltage is measured at a fixed delay after the microwave pulse. In Fig. 3a, ΔV_{out} is plotted against the magnetic field at step 1, after subtraction of the linear background (see Fig. 2b). For the case of applied MW power, a peak and a dip are observed at positions symmetrically around the center of the step, with a height equal to half the step size. The amplitude of the peaks and dips decreases with decreasing microwave power (data not shown) and the position of the peaks depends on f_{MW} . We have performed the same measurements at qubit step 2 and we obtained similar results. For large power, we have also observed two photon peaks (data not shown). In Fig. 3c the microwave frequency is plotted against half the separation in applied external flux between the peak and the dip. We did not reliably identify peaks and dips for $f_{\text{MW}} < 8.5$ GHz and therefore we could not determine Δ . A linear fit of the peak positions gives a value of the persistent current $I_p = 870 \pm 30$ nA, which is in agreement with the value that can be

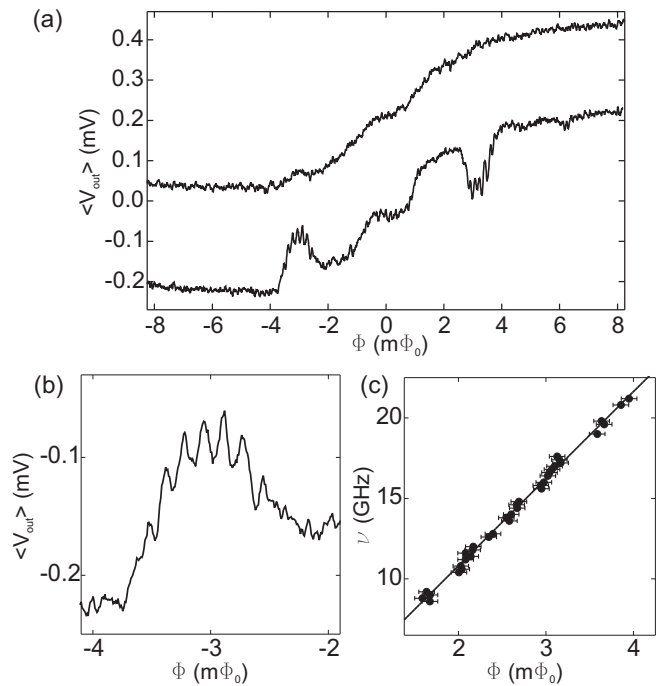


FIG. 3: (a) Spectroscopy measurements at $f_{\text{MW}} = 17$ GHz, for $T_{\text{MW}} = 1$ s, $T_d = 0$ s, and $T_m = 2$ s, for no applied MW power (top curve) and for $P_{\text{MW}} = 9$ dBm (bottom curve). The readout circuit has a resonance frequency of 840 MHz and is operated at 855 MHz, using a AC amplitude such that $\epsilon_0 = 0.5$. The data is plotted after averaging over flux intervals of 49 ± 0 and 42 ± 0 , respectively, and the two curves are offset for clarity. (b) A plot of the data in (a) in the region of the spectroscopy peak. (c) f_{MW} vs half the peak-dip separation (dots) and a linear fit through the origin (continuous line).

estimated from the height of the qubit step.

Both the spectroscopy peaks and dips display a weak modulation of the signal amplitude. This modulation is periodic with the applied magnetic field (see Fig. 3b). The period is the same in the peak and the dip and it does not depend on the microwave frequency and power. The position of the individual subpeaks changes linearly with f_{MW} , following the peaks and dips in which they are contained. The qubit energy separation, corresponding to the period of the sub-peaks $\Delta f = 0.1 = 1/\Delta \Phi = 1/\Delta \Phi = 880 \pm 130$ MHz; this is equal to the resonance frequency of the SQUID, within the determination error. This suggests that the observed substructure originates from transitions between the energy levels of the coupled qubit-SQUID system. The curves in Fig. 3a show a region, in the center of the step, characterized by a different slope. This region has a width and slope dependent on the amplitude of the circuit driving.

In Fig. 4 the data on the relaxation time measured at qubit step 1 for a level separation of 17 GHz is shown. We have measured this spectroscopy peak with the same T_r , T_{MW} and T_m , but with different delay times T_d . We

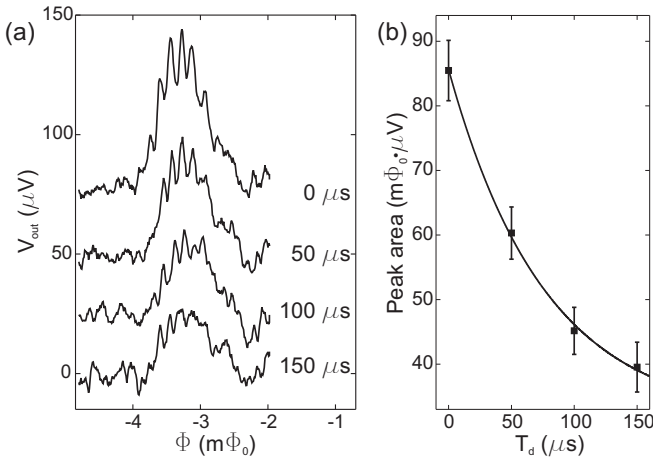


FIG. 4: (a) Spectroscopy peak at 17 GHz measured for 4 different values of the delay time between the qubit excitation pulse and the measurement pulse (plotted data is averaged over $\Phi = 56.2^\circ$). (b) The spectroscopy peaks areas plotted vs the delay time and a fit with an exponential decay dependence.

observe that the amplitude of the peak decreases with the increase in T_d , due to qubit relaxation (see Fig. 4a). The area of the Lorentzian curves fitting the peaks is plotted versus the delay time in Fig. 4b. A fit with an exponential decay gives the value of the relaxation time $T_1 = 77 \pm 12$ s. The obtained value of the relaxation time was independent of the measurement at either peak or dip and of the applied microwave power.

The output voltage noise level at the output of the amplification chain was $\sqrt{V_{\text{noise}}^2 + V_{\text{qubit}}^2} = 4$ V = $\text{Hz}^{1/2}$ and the output voltage difference corresponding to the 2 qubit states was $V_{\text{qubit}} = 800$ μV . A simple analysis shows that for an optimal integration time $T_m = 1.26 T_1$, the signal to noise ratio is $(S/N)_{\text{max}} = 11$, corresponding to a measurement fidelity of 70%. In this experiment, the flux-voltage conversion was degraded by the SQUID junctions asymmetry. Further improvement of the detection efficiency is possible by better impedance matching of the detection circuit to the amplifier and improvement of the amplifier noise. The estimated noise temperature of the amplification circuit was $T_n = 20$ K. The use of an optimized SQUID amplifier [17] combined with an amplification stage at 4.2 K would reduce the noise temperature to $T_n < 100$ mK, with a proportional reduction in measurement time.

In conclusion, we have implemented a new method for the readout of flux qubits, which eliminates the disadvantages of the strongly dissipative state associated with

the switching of a Josephson junction to the voltage state. Using this method, we have measured the spectroscopy and the relaxation time of a PCQ. The measurement has high efficiency and further improvement is possible, by optimizing the measurement circuit. This detector can be used for experimental studies of the relation between quantum measurement and decoherence, as well as for correlation measurements on 2 qubits.

We thank Alexander ter Haar and Hannes Maier for discussions. This work was supported by the Dutch Organization for Fundamental Research on Matter (FOM), the European Union SQUID project, and the U.S. Army Research Office (grant DAAD 19-00-1-0548).

- [1] M. A. Nielsen and I. L. Chuang, *Quantum Computation and Quantum Information* (Cambridge University Press, 2000).
- [2] Y. Nakamura, Y. A. Pashkin, and J. S. Tsai, *Nature* **398**, 786 (1999).
- [3] D. Vion, A. Aassime, A. Cottet, P. Joyez, H. Pothier, C. Urbina, D. Esteve, and M. H. Devoret, *Science* **296**, 886 (2002).
- [4] Y. Yu, S.-Y. Han, X. Chu, S.-I. Chu, and Z. Wang, *Science* **296**, 889 (2002).
- [5] J. M. Martinis, S. Nam, J. Aumentado, and C. Urbina, *Phys. Rev. Lett.* **89**, 117901 (2002).
- [6] I. Chiorescu, Y. Nakamura, C. J. P. M. Harmans, and J. E. Mooij, *Science* **299**, 1869 (2003).
- [7] T. D. Durt, D. Gunnarsson, K. B. Lædje, R. J. Schoelkopf, and P. Delsing, *cond-mat/0305433* (2003).
- [8] Y. A. Pashkin, T. Yamamoto, O. Astafyev, Y. Nakamura, D. V. Averin, and J. S. Tsai, *Nature* **421**, 823 (2003).
- [9] T. Yamamoto, Y. A. Pashkin, O. Astafyev, Y. Nakamura, and J. S. Tsai, *Nature* **425**, 941 (2003).
- [10] J. B. Maier, F. G. Paauw, A. C. J. ter Haar, C. J. P. M. Harmans, and J. M. Mooij, *cond-mat/0308192* (2003).
- [11] A. J. Berkley, H. X. Xu, R. C. Ramaswami, M. A. Gubrud, F. W. Strauch, P. R. Johnson, J. R. Anderson, A. J. D. Ragh, C. J. Lobb, and F. C. W. Ellsworth, *Science* **300**, 1548 (2003).
- [12] R. J. Schoelkopf, P. W. Ahlgren, A. A. Kozhevnikov, P. Delsing, and D. E. P. Roper, *Science* **280**, 1238 (1998).
- [13] A. B. Zorin, *Phys. Rev. Lett.* **86**, 3388 (2001).
- [14] J. E. Mooij, T. P. Orlando, L. Levitov, L. Tian, C. H. van der Wal, and S. Lloyd, *Science* **285**, 1036 (1999).
- [15] A. Lupascu, et al., *in preparation*.
- [16] C. H. van der Wal, A. C. J. ter Haar, F. K. W. Wilhelm, R. N. Schouten, C. J. P. M. Harmans, T. P. Orlando, S. Lloyd, and J. E. Mooij, *Science* **290**, 773 (2000).
- [17] M. Mück, J. B. Kycia, and J. Clarke, *Appl. Phys. Lett.* **78**, 967 (2001).